Polymer Vol. 37 No. 4, pp. 573–579, 1996

0032-3861/96/$15.00 + 0.00

Structure and gas permeability of microporous films prepared by biaxial drawing of β-form polypropylene

Feng Chu and Yoshiharu Kimura*
Department of Polymer Science and Engineering, Kyoto Institute of Technology, Matsugasaki, Kyoto 606, Japan
(Received 18 May 1995; revised 22 June 1995)

Polypropylene (PP) films with high β-crystal content were drawn biaxially under various conditions to obtain highly porous films. Their pore size distribution and pore volume, measured by the mercury intrusion method, were found to depend on the draw ratio. Wide-angle X-ray diffraction of the drawn films in edge view showed that the α and β crystals are oriented in directions parallel and perpendicular to the drawing directions, respectively. The morphologies of the films drawn to various draw ratios could be explained by a two-step mechanism that involves the deformation of lamellar blocks and the formation of microfibrils. The oxygen and carbon dioxide permeabilities of these films were also measured and compared with those of films drawn uniaxially at constant width. The high permeability coefficients (of the order of 10^5 Barrer) suggested that the biaxially drawn films can be used as gas exchange membranes.

(Keywords: β-form polypropylene; biaxial drawing; micropore formation)

INTRODUCTION

The deformation of β-form polypropylene (β-PP) has been an interesting subject of research because transformation from β to α or to smectic form with unusual micropore formation can be observed in the process of deformation[1]. As we reported in previous papers[2,3], highly porous films with porosity as high as 40 vol% could be obtained by cold drawing of β-PP films, although their pore size distribution was relatively wide. Pore formation was found to depend on the crystallization temperature (T_{cr}) when preparing the original β-PP film as well as the drawing temperature (T_{dr}). Based on detailed studies of the morphological and crystallographic changes of uniaxially drawn films, we have postulated a two-step mechanism for deformation and pore formation[3]: (1) breakage of the weak boundaries present between the lamellar blocks of β crystals to form micropores, and (2) enlargement of the micropores with microfibril formation. The porosity and the pore size distribution are, therefore, closely related to the stability of the β crystals and the lamellar dimensions in the original films. For further study of this interesting behaviour of β-PP, we examined biaxial drawing of β-PP films in which the collapse of pores by fibril packing may be avoided effectively. This paper reports the new results of crystal transformation and micropore formation of biaxially drawn β-PP films. In addition, the gas permeabilities of the porous films obtained by both biaxial and uniaxial drawing were investigated with the purpose of assessing their potential application as gas exchange membranes.

* To whom correspondence should be addressed

EXPERIMENTAL

Materials

Polypropylene pellets (melt index = 14) blended with 0.1 wt% of a newly developed β-nucleator (NJSTAR) were supplied by New Japan Chemical Co. Ltd (Kyoto)[4]. β-PP films with a thickness of ca. 0.2 mm were prepared by cooling the hot-pressed PP in air or at a defined T_{cr}. Their relative β-crystal content was higher than 90% as calculated by the K value[1]. The resultant β-PP films were then subjected to biaxial drawing up to a predetermined draw ratio (λ) at a defined drawing temperature (T_{dr}).

Measurements

The pore size and pore size distribution were determined by the mercury intrusion method using a Porosimeter-2000 (Carlo Erba Instruments, Italy). The porosity was also measured by the oil absorption method using salad oil as described in the previous paper[1]. Scanning electron microscopy (SEM) was done on a JSM 840 microscope with gold-coated sample. Wide-angle X-ray diffraction (WAXD) was carried out on an X-ray diffractometer of JDX 7E type (JEOL). The X-rays were generated at 40 kV and 20 mA, and Ni-filtered Cu Kα radiation was used. The exposure time was 4 h.

The gas permeabilities of the films for O_2 and CO_2 were measured by the vacuum method using an apparatus made by Rigaku Seiki Industrial Co.

(Tokyo)[4]. The permeability coefficient (P) was determined from the slope of the pressure change (dp/dt) at steady state. The diffusion coefficient (D) was estimated from the time lag θ in permeation by using the equation $D = d^2/6\theta$, where d denotes the thickness of the film.

RESULTS AND DISCUSSION

Pore size distribution of the biaxially drawn film

The β-PP film, which was prepared by cooling the hot-pressed PP slowly at room temperature, consisted of stable β crystals like the one prepared at $T_{cr} = 110°C$[2] and could be biaxially drawn at temperatures higher than 110°C to produce a white porous film without neck formation. The pore size distribution of the biaxially drawn film obtained was measured by the mercury intrusion method. *Figure 1* shows typical results for films drawn to various draw ratios. It is clearly shown that the maximum pore size and pore size distribution increased with increasing draw ratio. From these data, the average pore size, surface area and pore volume were calculated and are summarized in *Table 1*. The film drawn to a small draw ratio of $\lambda = 1.2 \times 1.3$ had an average pore size of 336 Å and a pore volume of 21.4%. The average pore size increased progressively with increasing draw ratio and jumped when the draw ratio reached 2.2 × 2.3, while the porosity reached a plateau at $\lambda > 1.7 \times 1.8$. The film of $\lambda = 1.7 \times 1.8$ showed the highest porosity and surface area, with relatively homogenous pore size distribution.

Table 1 Pore size, surface area and porosity[a] of β-PP films[b] biaxially drawn at 125°C

Drawing ratio	Average pore radius (Å)	Surface area (m^2g^{-1})	Porosity (%)
1.2 × 1.3	336	27.2	21.4
1.3 × 1.5	352	29.8	25.5
1.7 × 1.8	392	57.7	38.1
2.1 × 2.2	624	35.9	37.5

[a] Measured by mercury intrusion porosimetry
[b] Original films were prepared by cooling in air

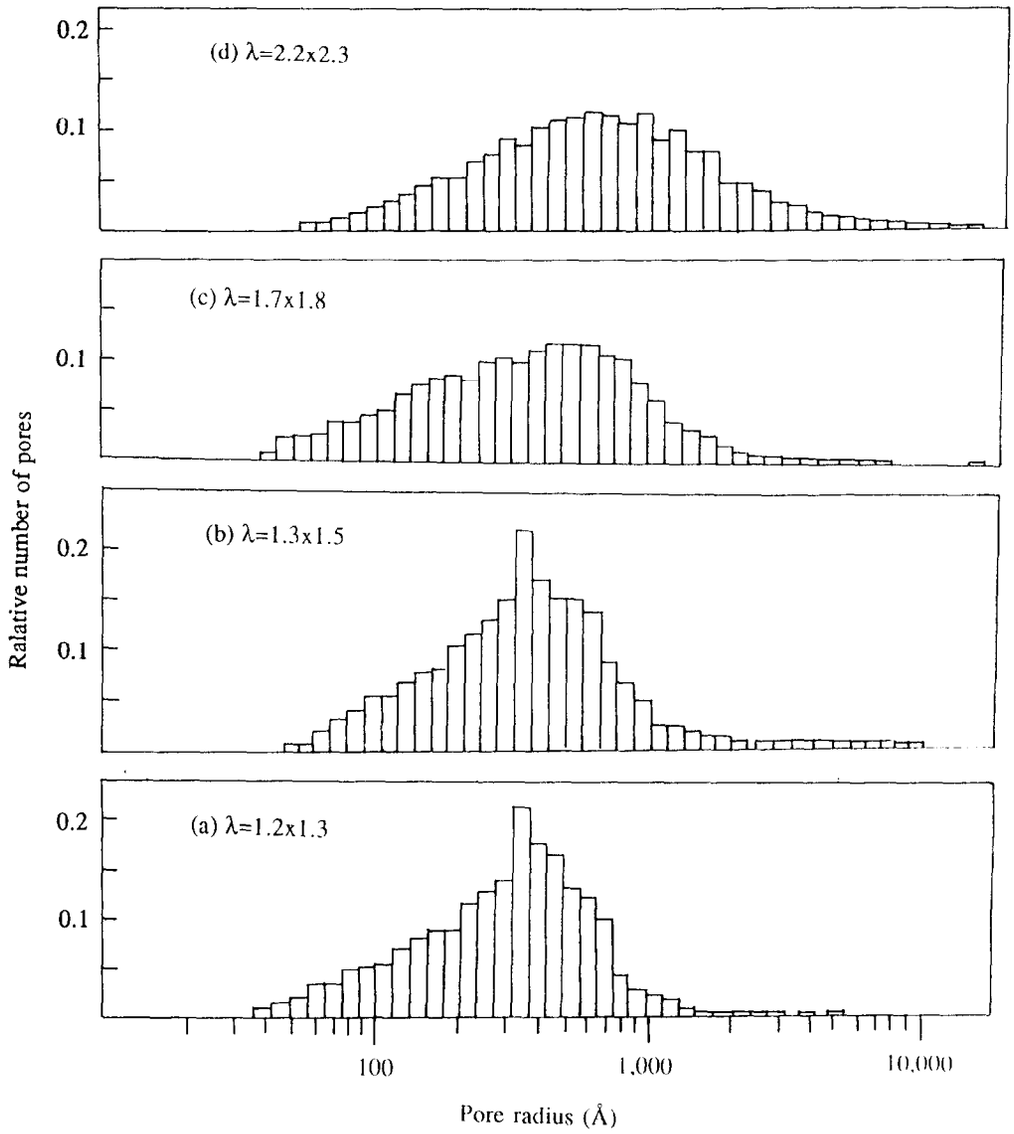

Figure 1 Pore size distributions of the biaxially drawn β-PP films measured by the mercury intrusion method: (a) $\lambda = 1.2 \times 1.3$, (b) $\lambda = 1.3 \times 1.5$, (c) $\lambda = 1.7 \times 1.8$, and (d) $\lambda = 2.2 \times 2.3$

Morphology

Figure 2 shows the SEM photographs of the surfaces of biaxially drawn films. In the film drawn to $\lambda = 1.2 \times 1.3$, many pores and cracks are distributed in the surface, with the flat regions keeping the original structure. This morphology may strongly support the mechanism[3] in which the weak boundaries between the lamellar blocks are deformed to form pores in the initial stage of drawing. At a higher draw ratio ($\lambda = 1.3 \times 1.5$), the film is further split into small blocks to form more pores between them. In the films drawn to $\lambda = 1.7 \times 1.8$ and 2.2×2.3, microfibril formation is clearly noted, as shown in *Figures 2c* and *2d*. The microfibrils seem to grow proportionally to the draw ratio, and the pores are homogeneously distributed between the crossed bundles of microfibrils. *Figure 3* shows the SEM of the films drawn to $\lambda = 1.7 \times 1.8$ and 2.2×2.3 in edge view. It clearly indicates that continuous microfibrils have grown and packed more densely with increasing draw ratio. This microfibril formation would cause bulk volume shrinkage and thinning of the films with the amount of continuous pores decreasing.

Crystallography

For analysis of the crystal transformation and orientation, WAXD of the biaxially drawn films was investigated. *Figure 4* shows typical results for the fully stretched samples in both through and edge views. In the through views, the diffractions due to β crystals are still strong, and the diffractions of α crystals are weak. In the edge view of the film drawn up to $\lambda = 1.7 \times 1.8$, the (1 1 0), (0 4 0) and (1 3 0) diffraction arcs due to the α crystals are shown in the equatorial region, together with the (3 0 0) diffraction due to the β crystals in the polar

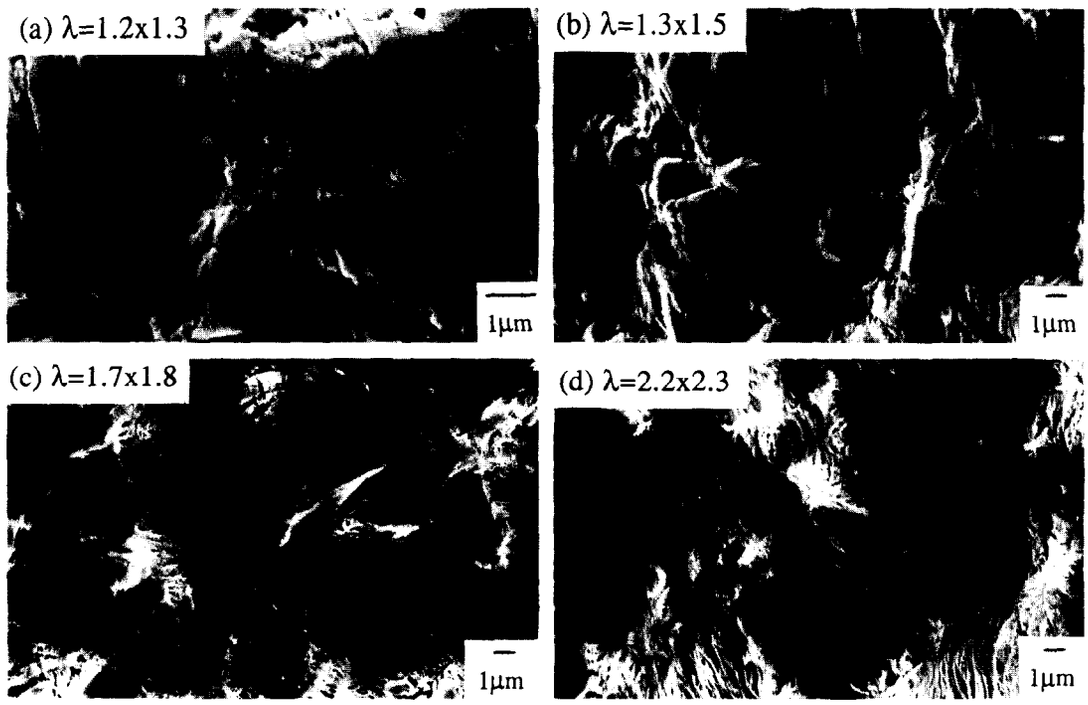

Figure 2 SEM photographs of the biaxially drawn β-PP films: (a) $\lambda = 1.2 \times 1.3$, (b) $\lambda = 1.3 \times 1.5$, (c) $\lambda = 1.7 \times 1.8$ and (d) $\lambda = 2.2 \times 2.3$

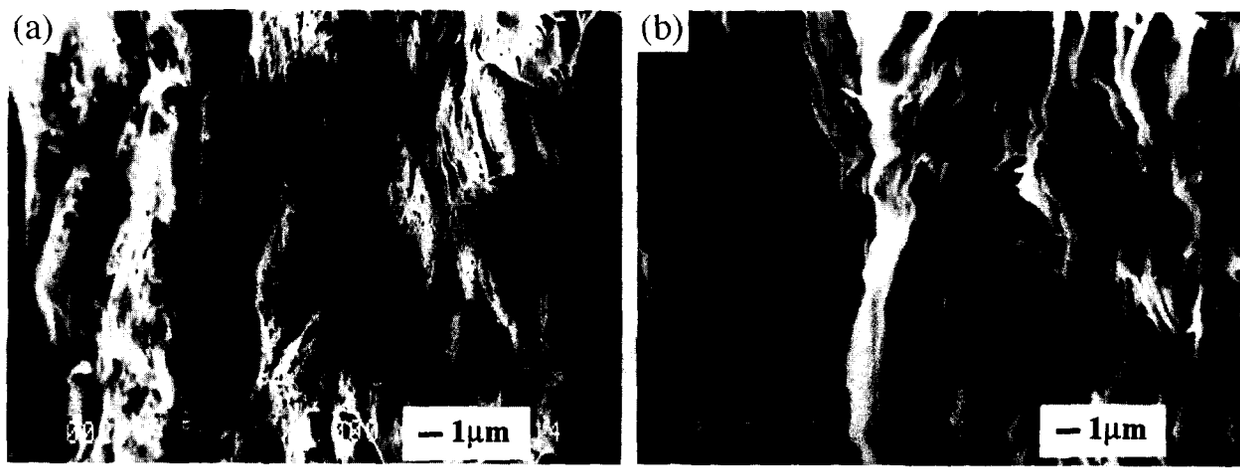

Figure 3 SEM photographs in edge view of the biaxially drawn films: (a) $\lambda = 1.7 \times 1.8$ and (b) $\lambda = 2.2 \times 2.3$

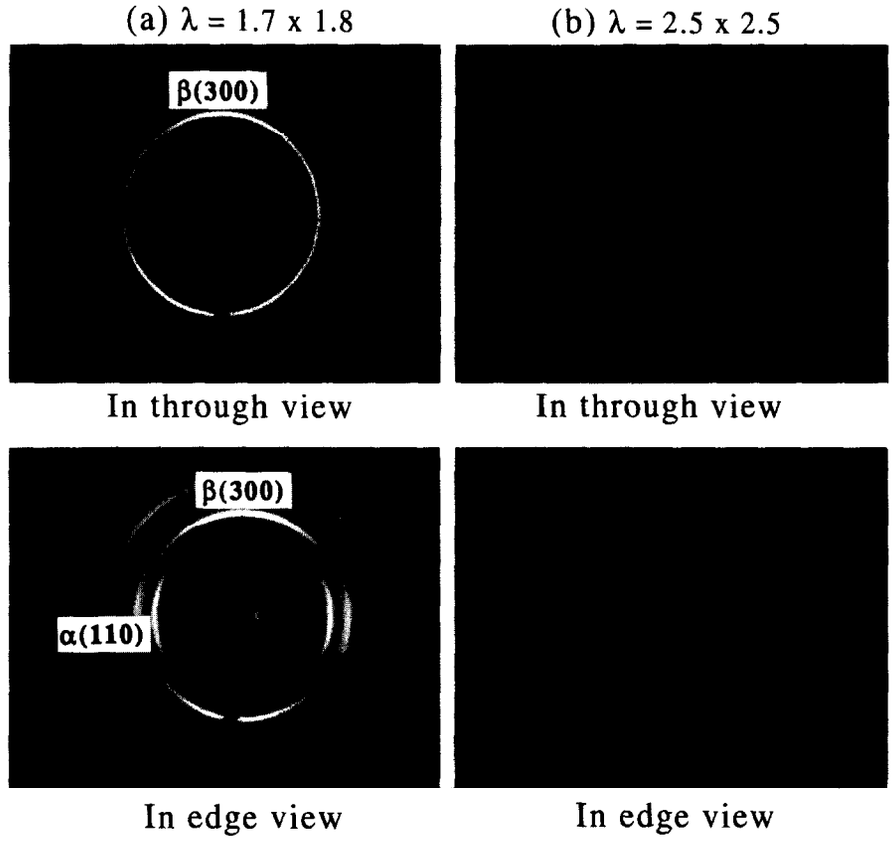

Figure 4 WAXD of the biaxially drawn β-PP films: (a) $\lambda = 1.7 \times 1.8$ and (b) $\lambda = 2.5 \times 2.5$

region. For the film drawn to $\lambda = 2.5 \times 2.5$, all three α diffraction arcs are concentrated into the equatorial region more closely, showing an improved orientation. This indicates that the α crystals are oriented in the drawing direction while the β crystals remain with orientation in the direction perpendicular to the drawing direction. This structure having α and β crystals in the opposite orientations may reflect the process of crystal transformation. As schematically represented in *Figure 5*, β crystals with *c* axis parallel to the drawing direction in the spherulites are first transformed into α crystals, and then those with *c* axis tilted to the drawing direction are involved in the transformation at a lower rate[1]. For crystals with *c* axis perpendicular to the drawing directions, crystal rotation may be retarded because the stretching stresses exerted on these crystals from the four directions counteract one another, as depicted by the arrows in *Figure 5*. Consequently, their crystal transformation was hindered, and they remained in the biaxially drawn sample with orientation perpendicular to the drawing direction. This result suggested that the orientation of β crystals is one of the important factors for the $\beta \rightarrow \alpha$ phase transformation during drawing[5–7], and that the β crystals with *c* axis tilted to the drawing direction should be rotated to the drawing direction prior to the transformation.

The sketches in *Figure 5* show the processes of lamellar deformation in which the β crystals are involved in biaxial drawing. The stretching stress exerted on the lamellae perpendicular to the drawing direction is along the molecular chains and allows chain unfolding, leading to phase transformation. As a consequence, the β crystals existing in these lamellae transform into α crystals in an earlier stage of drawing. On the other hand, the stress exerted on the lamellae parallel to the drawing direction is applied as shear stress on the molecular chains. These lamellae cannot move until the neighbouring lamellae's movement adds extra stress on them and the shear stresses become imbalanced. Therefore, the chain unfolding involving the phase transformation only occurs at large draw ratio.

Gas permeability of the drawn film

As a consequence of the existence of continuous micropores, the biaxially drawn β-PP films ought to have improved gas permeability. So, their gas permeability was measured by the vacuum method. The experimental results indicated that the O_2 permeability coefficients of biaxially drawn β-PP films reached as high as 10^5 Barrer*, while those of the original β-PP film and the biaxially drawn α-PP film were of the order of 0.1 and 10 Barrer, respectively. *Figure 6* shows the changes in permeability coefficient of O_2 and CO_2 with draw ratio or surface area expansion for the biaxially drawn films as compared with the change in porosity. At the early stage of drawing, both the permeability and porosity increased with increasing draw ratio, while at $\lambda > 1.7 \times 1.8$ the porosity levelled off and the permeability coefficient slightly decreased. This result may be related to a change in inner structure of the films by drawing, because it does not conform with the general principle that the gas permeability coefficient should be proportional to the pore radius and porosity if the pore

* 1 Barrer = 10^{-10} cm^3 cm/cm^2 s cmHg

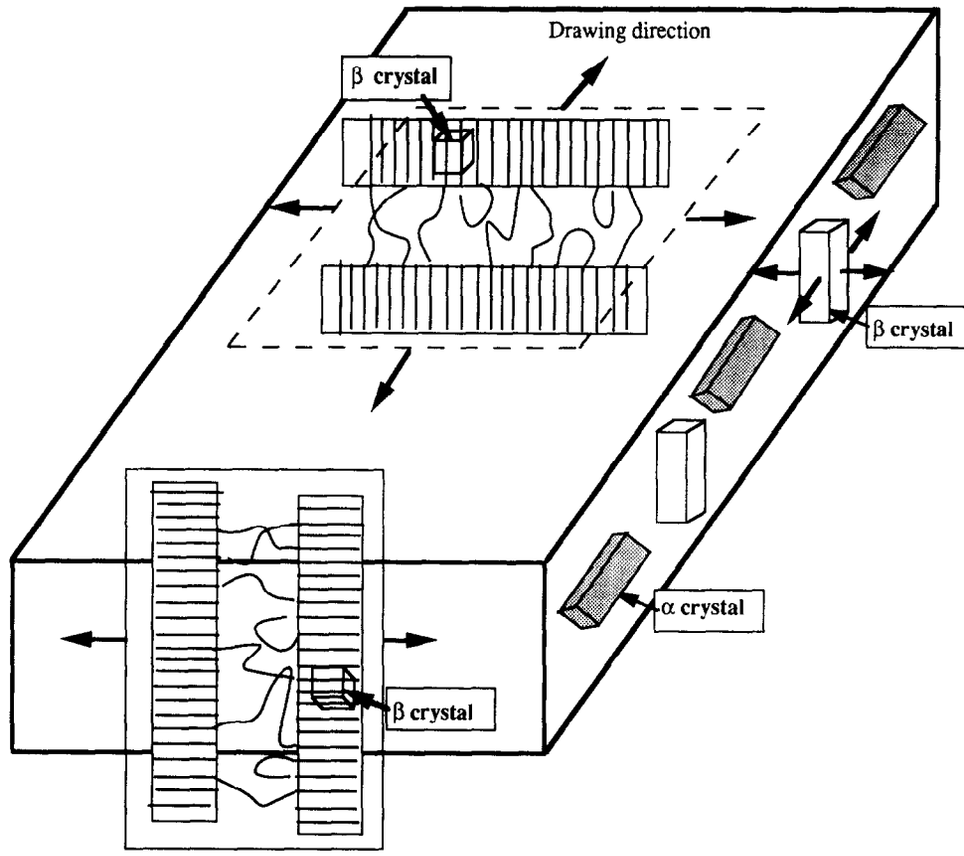

Figure 5 Schematic illustration of lamellar deformation and crystal orientation in a biaxially drawn β-PP film

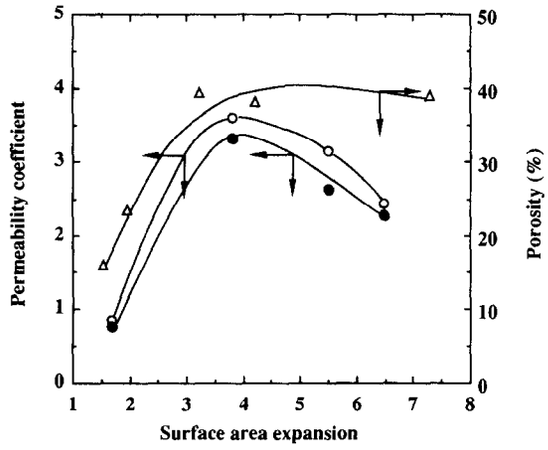

Figure 6 Effect of draw ratio (shown by the surface area expansion) on the permeability coefficients (10^5 Barrer) of O_2 (○) and CO_2 (●) and the porosity (△) of biaxially drawn β-PP films

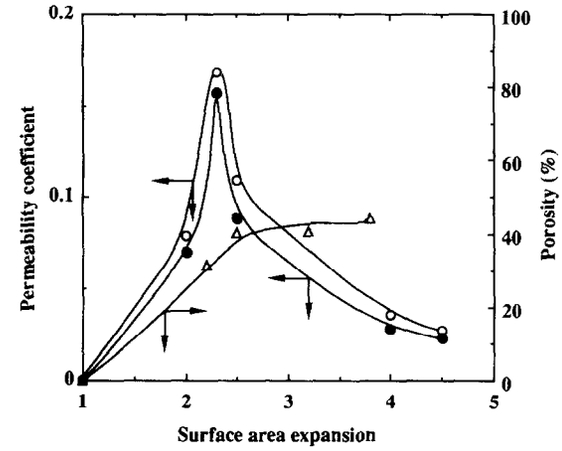

Figure 7 Effect of draw ratio on the permeability coefficients (10^5 Barrer) of O_2 (○) and CO_2 (●) and the porosity (△) for the β-PP films drawn uniaxially at constant width

distribution may be simulated by the integrated capillary model[8].

Because the biaxial drawing of β-PP film was difficult at lower temperature, uniaxial drawing was examined at constant width (the original width of the film was retained) to investigate the gas permeability of the drawn films in detail. *Figure 7* shows the changes in O_2 and CO_2 permeability coefficients and porosity with draw ratio for the uniaxially drawn films. It shows a tendency similar to *Figure 6* although the permeability coefficient is lower by one order of magnitude. When λ, i.e. surface area expansion, was larger than 2.5, the porosity reached a plateau whereas the gas permeability coefficients showed a large fall. At $\lambda = 4.0$, the permeability coefficient was even smaller than that of the film drawn to $\lambda = 2.0$.

Figure 8 indicates the effect of drawing temperature on the porosity and the O_2 permeability of the β-PP films drawn to $\lambda = 2.5$ uniaxially at constant width. It illustrates that the permeability coefficient decreased with increasing drawing temperature, while the porosity was constant up to 130°C and decreased above 130°C. For the film drawn at 150°C, the porosity became very low, and the permeability coefficient was as

low as the value of the drawn α-PP film. This suggested that pore formation of β-PP film was suppressed at 150°C.

The diffusion coefficient of O_2 for the drawn films also changed with drawing temperature. The change seems to be parallel with that of porosity in *Figure 8*. For the biaxially drawn films, in which most of the pores were continuous, the diffusion coefficients could not be determined because the time lag θ was too short.

It was found that the permeability coefficients for CO_2 are a little smaller than those for O_2 in most of the drawn β-PP films. This relation is contrary to that of α-PP and other polymer films, and should be attributed to the large number of pores present in the drawn β-PP films. If the porous structure of the film is suitable for the integrated capillary model, the permeability coefficient should be inversely proportional to the square root of the molecular weight of the permeant, and the ratio of permeability coefficient for O_2 to CO_2 should be 1.17. Since the present results were all around this value, it supported the view that the pores formed in the drawn β-PP films can be well simulated by the integrated capillary model.

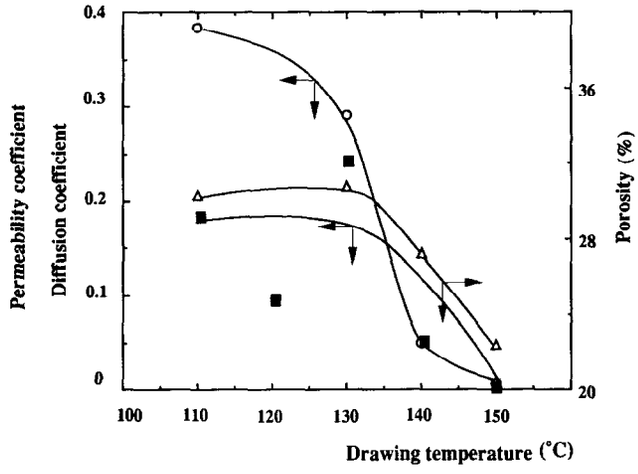

Figure 8 Effect of drawing temperature on the permeability coefficient (○) (10^5 Barrer) and diffusion coefficients (■) (10^{-5} cm^2 s^{-1}) of O_2 and porosity (△) for the β-PP films drawn uniaxially at constant width

Although the porosities of films drawn to draw ratios larger than 2.5 were not very different, their permeability coefficients decreased with draw ratio. This could be because their pore shape and distribution have become changed. *Figure 9* shows SEM photographs in edge view of the films drawn uniaxially at constant width. The film drawn to $\lambda = 2.0$ shows many large pores distributed throughout the films. These pores seem to be connected with each other to allow gas to diffuse inside the films. In the film drawn to $\lambda = 4.0$, however, most pores have collapsed with fibril propagation, and the structure has become closely packed. With this structure, gas diffusion would be hindered, particularly in the thickness direction. For the same reason, the large effect of drawing temperature on gas permeability shown in *Figure 8* is also ascribed to increased microfibril packing, which is induced by the faster crystal transformation of the β-PP at higher temperature. Therefore, it is understood that the thick stacking of microfibrils results in the fall of the gas permeability in spite of little change in porosity.

The micropores are formed more homogeneously in the biaxially drawn β-PP film, as demonstrated in *Figure 1*. However, a similar fall of the gas permeability coefficient was shown at larger draw ratios although it was much smaller than that in uniaxially drawn films. This may also be attributed to fibril propagation. Since the fibrils cannot be aligned in one direction by biaxial drawing, the collapse of pores is prohibited to slow the drop of gas permeability. The data shown above demonstrated that phase transformation, micropore formation and fibril formation are closely related with each other and that the gas permeability of drawn β-PP films can be adjusted by controlling the drawing conditions. Since the gas permeabilities of the drawn films are comparable to those of commercially available gas exchange membranes, the films may have potential applications as external membranes for oxygenators.

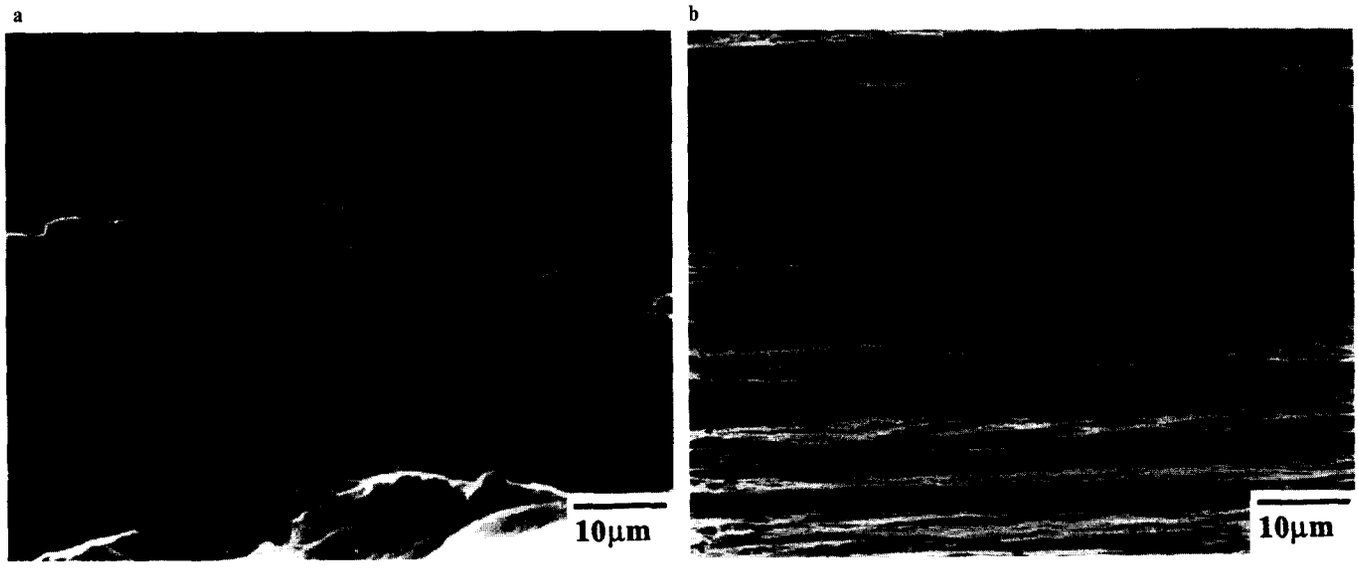

Figure 9 SEM photographs in edge view of the films drawn uniaxially at constant width at 130°C: (a) $\lambda = 2.0$ and (b) $\lambda = 4.0$

REFERENCES

1 Shi, G., Chu, F., Zhou, G. and Hang, Z. *Makromol. Chem.* 1989, **189**, 909
2 Chu, F., Yamaoka, T., Ide, H. and Kimura, Y. *Polymer* 1994, **35**, 3442
3 Chu, F., Yamaoka, T. and Kimura, Y. *Polymer* 1995, **36**, 2523
4 Ikeda, N., Yoshimura, M., Mizoguchi, K., Kitagawa, H. and Kawashima, M. Japan Kokai H5-262936, 1993
5 Asano, T. and Fujiwara, Y. *Polymer* 1978, **19**, 99
6 Asano, T., Fujiwara, Y. and Yoshida, T. *Polym. J.* 1979, **11**, 383
7 Yoshida, T., Fujiwara, Y. and Asano, T. *Polymer* 1983, **24**, 925
8 'Kagaku Binran, Ouyou Kagaku Hen, II' (in Japanese), Maruzen, Tokyo, 1986, p. 1175
9 Tsuji, T., Suma, K., Tanishita, K., Fukazawa, H., Kanno, M., Hasegawa, H. and Takashi, A. *Trans. Am. Soc. Artif. Intern. Organs* 1981, **27**, 280